22. D. A. Maclean, H.-N. Ng, J. E. Greedan, *J. Solid State Chem.* **30**, 35 (1979); M. Marezio, J. P. Remeika, P. D. Dernier, *Acta Crystallog. Sect. B* **26**, 300 (1970).
23. H. B. Bowman, *Mineral. Mag.* **15**, 156 (1908); T. J. White, R. L. Segall, J. C. Barry, J. L. Hutchison, *Acta Cryst.* **B41**, 93 (1985).
24. H. D. Megaw, *Crystal Structures: A Working Approach* (Saunders, Philadelphia, 1973).
25. The sequence of phase transitions (*Pm3m* to *P4/mbm* to *Pbnm*) is somewhat arbitrary and chosen only for convenience. In the transition from *Pm3m* to *Pbnm*, there are a limited number of possible intermediate structures [see (*1*)]. Our conclusions hold for the general transition sequence (in terms of point group symmetry) from *m3m* to *4/mmm* to *mmm*.
26. In situ high-temperature TEM study on structural phase transitions in $NaNbO_3$ has shown that the two twin-types, {141} and {101} (equivalent to the {112} and {110} twinning, respectively, in $MgSiO_3$), are consistent with our geometrical interpretation and are associated with cubic-tetragonal and tetragonal-orthorhombic transitions, respectively; F. Guyot and Y. Wang, in preparation.
27. For the transition from cubic to tetragonal (*Pm3m* to *P4/mbm*), theory [J. Sapriel, *Phys. Rev. B* **12**, 5128 (1975)] predicts that there are three possible twin relations and six permissible domain wall orientations: $(110)_c$, $(011)_c$, $(101)_c$, $(\bar{1}01)_c$, $(1\bar{1}0)_c$, and $(10\bar{1})_c$. These are approximately either (100), (010), or {112} planes in the orthorhombic structure. For the transition from tetragonal to orthorhombic (*P4/mbm* to *Pbnm*), there are two possible twin relations and two permissible domain wall orientations $\{110\}_{tetr}$ (approximately orthorhombic {110}).
28. G. H. Wolf and M. S. T. Bukowinski, in *High-Pressure Research in Mineral Physics* (Akimoto volume), M. H. Manghnani and Y. Syono, Eds. (American Geophysical Union, Washington, DC, 1987), pp. 313–331.
29. We thank T. Gasparik and D. J. Weidner for advice on cell assemblies and X. Liu, Y. Kudoh, J. P. Poirier, R. J. Reeder, E. Salje, and D. J. Weidner for stimulating discussions. We also thank D. Presnall for the enstatite starting material and Y. Kudoh for a preprint of (*14*). The High-Pressure Laboratory is supported by the National Science Foundation (NSF) grant EAR 86-07105 and the State University of New York at Stony Brook. The electron microscopy was performed with the use of a JEOL 200CX transmission electron microscope under the supervision of R. J. Reeder. The research was also supported by NSF grants EAR 88-17097 and 88-04087.

16 November 1989; accepted 23 March 1990

GT-1 Binding Site Confers Light Responsive Expression in Transgenic Tobacco

ERIC LAM* AND NAM-HAI CHUA

Light-dependent expression of *rbcS*, the gene encoding the small subunit of ribulose-1,5-bisphosphate carboxylase, which is the key enzyme involved in carbon fixation in higher plants, is regulated at the transcriptional level. Sequence analysis of the gene has uncovered a conserved GT motif in the −150 to −100 region of many *rbcS* promoters. This motif serves as the binding site of a nuclear factor, designated GT-1. Analysis of site-specific mutants of pea *rbcS-3A* promoter demonstrated that GT-1 binding in vitro is correlated with light-responsive expression of the *rbcS* promoter in transgenic plants. However, it is not known whether factors other than GT-1 might also be required for activation of transcription by light. A synthetic tetramer of box II (TGTGTGGTTAATATG), the GT-1 binding site located between −152 to −138 of the *rbcS-3A* promoter, inserted upstream of a truncated cauliflower mosaic virus 35*S* promoter is sufficient to confer expression in leaves of transgenic tobacco. This expression occurs principally in chloroplast-containing cells, is induced by light, and is correlated with the ability of box II to bind GT-1 in vitro. The data show that the binding site for GT-1 is likely to be a part of the molecular light switch for *rbcS* activation.

THE ELUCIDATION OF THE MOLECULAR mechanisms for light-responsive gene expression is an important step toward understanding photomorphogenesis. While the mechanism by which the photoreceptor phytochrome transmits its signal remains unknown, analyses of light-regulated genes in transgenic plants have demonstrated that the promoter region of many of these genes harbors DNA elements for light-responsive expression (*1, 2*). In addition, the promoters of several *rbcS* (genes that encode the small subunit of ribulose-1,5-bisphosphate carboxylase) direct expression preferentially in chloroplast-containing cells (*3, 4*). Thus, the promoter for *rbcS* contains genetic information for light responsiveness as well as for cell specificity. In vitro studies with plant nuclear extracts have identified GT-1 (*5*) and a G-box factor (*6*) as nuclear proteins that interact with light-responsive promoters. The binding of GT-1 has been mapped to conserved elements termed box II and box III in the upstream regions of *rbcS* promoters from many dicotyledonous species (*1, 5*). Site-specific mutations in box II and box III result in a loss of GT-1 binding in vitro and are correlated with the attenuation of the *rbcS-3A* promoter function in vivo (*7*). In addition, a 116–base pair (bp) fragment, from −166 to −50 of *rbcS-3A*, containing box II (5′-GTGTGGTTAATATG-3′) and box III (5′-ATCATTTTCACT-3′), is able to confer light responsiveness to the cauliflower mosaic virus (CaMV) 35*S* promoter truncated at −46 (*8*). These studies show that GT-1 binding is likely to be necessary for the light-dependent activation process under our assay conditions. However, whether GT-1 alone is sufficient or binding of additional factors to the 116-bp fragment is also required for light-responsive gene

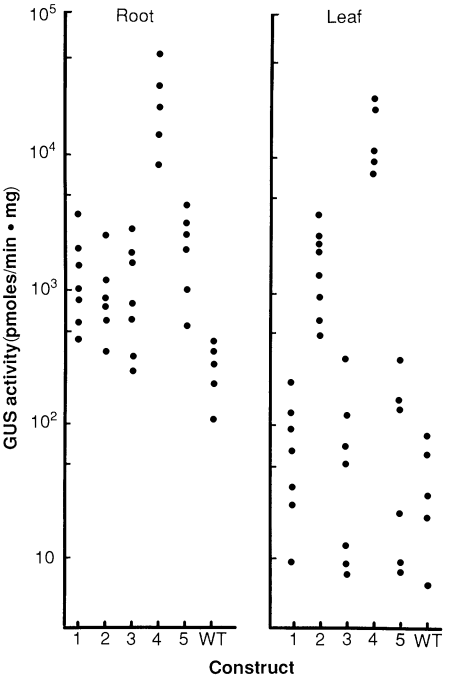

Fig. 1. Activity of *rbcS-3A* box II and *as-1* tetramers in transgenic tobacco. Activity is expressed as picomoles of 4-methylumbelliferone produced per minute per milligram protein, with 4-methyl umbelliferyl glucuronide as substrate (*15*). Data from five to ten independent transgenic plants for each construct are shown. *RbcS-3A* box II sequence (−152 to −138) is TGTGTGGTTAATATG and its mutant sequence is TGTGTCCTTAATATG, with the mutated bases underlined (*12*). Activation sequence-1 (*as-1*) is derived from the −82 to −62 region of the CaMV 35*S* promoter upstream sequence and has the sequence CTGACGTAAGGGATGACGCAC. The sequence of its mutant derivative is CTGCTGTAAGGGATCTCGCAC, with the mutated bases underlined (*13*). Tetramers of box II and its mutant derivative are designated 4II and 4IIm, respectively. Tetramers of *as-1* and its mutant derivative are designated 4AS1 and 4AS1m, respectively. All tetramers were synthesized with a Hind III site on the 5′ end and an Xho I site on the 3′ end. These sites were used for cloning of the tetramers into the X-GUS-90 vector, as described in the text. Construct 1, X-GUS-90; construct 2, 4II-90; construct 3, 4IIm-90; construct 4, 4AS1-90; construct 5, AS1m-90; WT, nontransformed tobacco. Each dot represents the activity of an independent transgenic plant.

Laboratory of Plant Molecular Biology, Rockefeller University, New York, NY 10021.

*To whom correspondence should be addressed at: AgBiotech Center, Waksman Institute of Microbiology, Rutgers State University, Piscataway, NJ 08855.

expression remains unresolved.

To demonstrate the positive function of GT-1 in vivo, we fused a synthetic *rbcS-3A* box II tetramer to the −90 derivative of the CaMV 35*S* promoter [that is, the X-GUS-90 vector (*9*)] to generate the construct 4II-90. This truncated derivative of the CaMV 35*S* promoter has been shown to confer expression preferentially in root (*10, 11*). The coding sequence for the *Escherichia coli* β-glucuronidase (GUS) gene was fused 3′ to the 35*S* promoter and served as the reporter gene. As a negative control, we fused a tetramer of mutant box II, in which the two G's at positions −147 and −146 were altered to C's, to X-GUS-90 (4IIm-90). These mutations reduced the binding affinity of GT-1 by at least ten times (*12*). For comparison, wild-type and mutant binding sites (*as-1* and *as-1m*) for another characterized plant nuclear factor, activation sequence factor-1 (ASF-1) (*13*), were also fused to the X-GUS-90 vector, forming the constructs 4AS1-90 and 4AS1m-90. These constructs were transformed into *Nicotiana tabacum* (cv. SR1) by the use of *Agrobacterium tumefaciens* (*14*), and the expression of the artificial promoters was assayed by measuring the GUS enzyme activity in both root and leaf extracts (*15*). The X-GUS-90 vector, as reported earlier (*10, 11*), had significant expression above background in root but not in leaf (Fig. 1). This root-specific activity was enhanced significantly by the *as-1* tetramer. In contrast, the box II tetramer did not give any significant enhancement of GUS activity in root. However, in leaf, GUS expression was observed with both wild-type box II and *as-1* tetramers, with the latter being about nine times more active. For both tetramers, mutations that severely decrease binding of their cognate factor in vitro (*12, 13*) also reduce drastically the ability of the tetramers to potentiate transcription from the truncated 35S promoter.

We then examined the effects of modulation by light on the artificial promoters 4II-90 and 4AS1-90 (Fig. 2). Transgenic plants were grown in a 16-hour light and 8-hour dark cycle or constant darkness for 2 days. Leaves were collected in the afternoon of the second day and the levels of transgene expression were compared by 3′ S1 nuclease protection assays. The X-GUS-90 vector contains a reference gene comprised of a CaMV 35*S* upstream fragment (−941 to +8) fused to the coding sequence of bacterial chloramphenicol acetyl transferase (CAT). The 3′ polyadenylation sequences for the test (that is, the GUS) gene and the reference gene were derived from the corresponding regions of pea *rbcS-3C* and *rbcS-E9*, respectively (*16*). Since these 3′ regions have homologous sequences, we can compare quantitatively the test and reference gene transcripts with the same S1 probe. Expression of the 4II-90 construct was dependent on light, whereas the expression of 4AS1-90 construct was slightly higher in the dark than in the light. The reference CAT gene in both constructs appears to be expressed at similar levels in both light and dark.

We have also examined the cell type specificity of the artificial promoters in construct 4II-90 and 4AS1-90 by histochemical localization of the GUS gene product in transgenic plants. In leaf, the box II tetramer conferred expression predominantly in chloroplast-containing cells (that is, the mesophyll cells and the chlorenchyma), whereas the *as-1* tetramer was active in diverse cell types (Fig. 3). We cannot be certain whether the 4II-90 construct is expressed in all chloroplast-containing cells; however, we have not observed expression of this promoter in leaf cells that do not contain chloroplasts, such as the vascular elements. Both mutant binding site constructs, 4IIm-90 and 4AS1m-90, did not show significant staining in leaf tissues. In root, the 4II-90 construct showed staining mainly in the tip region (Fig. 3E). This expression pattern is indistinguishable from that of the X-GUS-90 vector alone (*11*) or the 4IIm-90 construct, suggesting that the box II tetramer is inactive in root. In contrast, the *as-1* tetramer gave extensive expression in all portions of the root (Fig. 3F).

Our data show that the tetramer of *rbcS-3A* box II, a binding site for the nuclear factor GT-1, can confer light-responsive and tissue-specific expression on a heterologous promoter in vivo. Quantitation of expression as determined by S1 nuclease protection assays shows that expression from this synthetic promoter is about 10 to 20% of that from the *rbcS-3A* promoter (*17*). A mutant box II tetramer that is defective in GT-1 binding is unable to confer significant expression on the same promoter. These data provide indirect evidence for the positive function of GT-1 in the light-activation process. Previous site-specific mutagenesis studies have implicated box II and box III as positive elements (*7*), and have shown that a trimer of box II, when inserted between the CaMV 35*S* enhancer and promoter, can attenuate expression of the CaMV 35*S* promoter in the dark (*18*). Although these data suggested that the box II trimer can function as a negative element, it was not clear that the reduced expression in the dark was due to GT-1 binding, as site-specific mutants of box II were not included for a negative control. If GT-1 and box II are involved in both activation of *rbcS* in the light and repression in the dark, the mode of action of GT-1 may be explained by one of the models in Fig. 4. In models A and B, GT-1 interacts with either a positive factor (P) in the light or negative factor (N) in the dark. Neither P nor N bind DNA on their

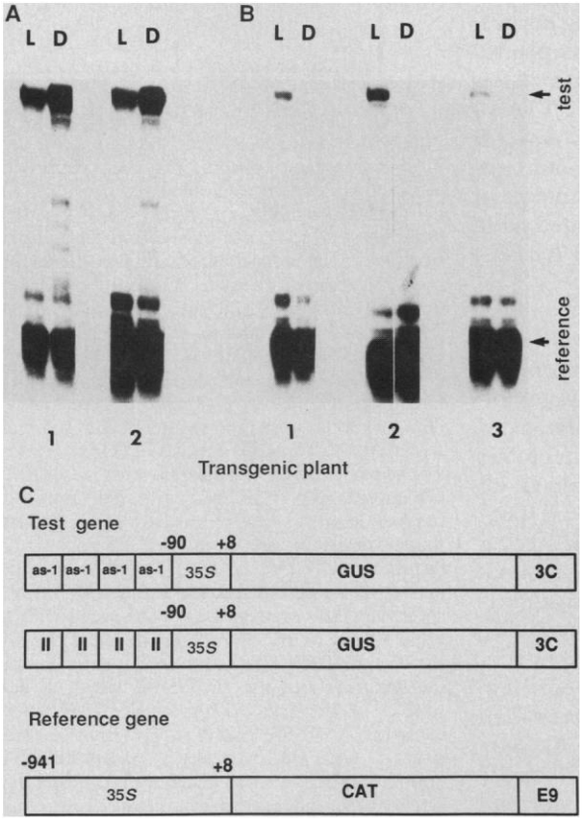

Fig. 2. Expression of synthetic promoters containing *as-1* or box II tetramers in transgenic tobacco. Five to ten independent transgenic plants with constructs 4AS1-90 or 4II-90 were assayed. Leaves from mature transgenic tobacco plants were collected in the light (L) or after transferring into dark boxes for 2 days (D). Total RNA (20 μg per lane) was analyzed by 3′ S1 nuclease digestion with a probe derived from the pea *rbcS-3C* 3′ region (*16*). Results from two and three representative plants are shown for constructs 4AS1-90 (**A**) and 4II-90 (**B**), respectively. Transcripts from the test gene (GUS) are expected to give protected bands of about 230 bases and those from the reference gene (CAT) about 89 bases (*16*). The constructs 4AS1-90, 4II-90, and reference gene are diagrammed in (**C**). Methods for tobacco transformation, RNA preparation, and S1 nuclease protection analyses have been described (*7, 14, 16, 18*).

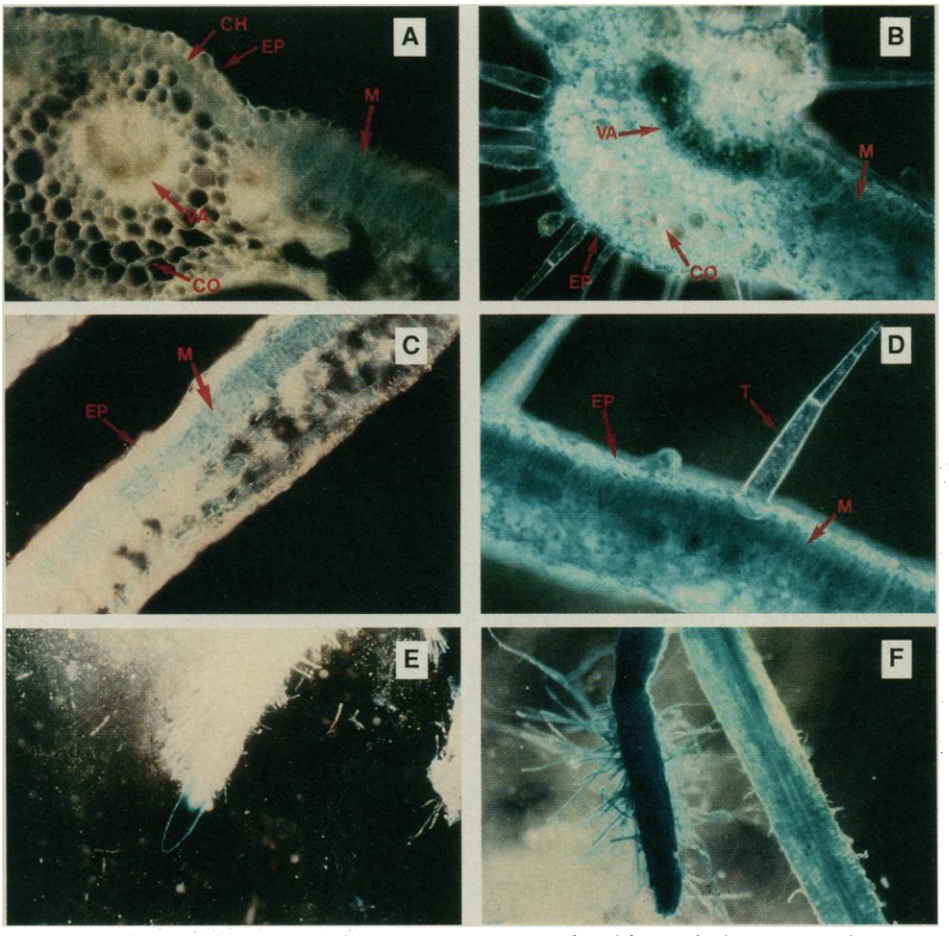

Fig. 3. Histochemical localization of expression patterns conferred by synthetic promoter elements. Hand sections of leaves and roots from representative transgenic tobacco containing the 4II-90 (**A, C, E**) and the 4AS1-90 (**B, D, F**) constructs are shown. Histochemical localization of GUS gene product was as described (*9*). Cell types were assigned as in (*3*). A and B, the mid-vein section of a tobacco leaf; C and D, the lamina portions; E and F, roots. CH, Chlorenchyma cell layer; VA, vascular elements; CO, collenchyma; EP, epidermis; M, mesophyll cells; T, trichome.

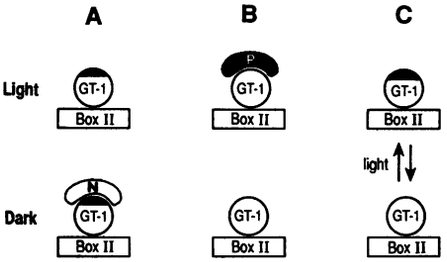

Fig. 4. Models for light activation of transcription mediated by GT-1 binding to box II. In (**A**) to (**C**) the *rbcS-3A* box II sequence is depicted as a rectangle and the DNA-binding protein, GT-1, is represented as a sphere. Shaded portions represent either activation domains or regions that can interact with other classes of factors to activate transcription. In (A) a negative regulator N is shown to bind to GT-1 in the dark and effectively mask the activation domain. In (B), GT-1 does not contain any activation domain of its own. However, in the light, a factor P with an activation domain binds to GT-1 and thereby activates transcription from the adjacent promoter. In (C), GT-1 is shown to undergo reversible modification during or after the transition between light and darkness. The end result of the modification is that a region of GT-1 becomes functional as an activation domain only in the light, while the DNA-binding properties of GT-1 remain unaffected. The size and shape of the various participants in the above model were idealized for ease of presentation.

own, and GT-1 binding to box II is independent of light. These two models are analogous to the interaction between the yeast factors GAL80 and GAL4, where GAL4 is a positive, DNA-binding transcription factor with an activation domain, and GAL80 interacts with GAL4 to inhibit trans-activation but not DNA binding (*19*). The third model, C, suggests that GT-1 may exist in two different states. GT-1 is functionally competent in trans-activation in the light but not in the dark; however, its DNA-binding property remains unaltered under both conditions. This model is similar to that suggested for the yeast heat shock transcription factor (*20*). The three models all incorporate the observation that DNA-binding activity of GT-1 is present in nuclear extracts from both light-grown and dark-adapted plants (*5, 12*).

ASF-1 binds to the −82 to −62 region (that is, the *as-1* site) of the CaMV 35*S* promoter (*13*). A −90 derivative of the CaMV 35*S* promoter shows root-specific expression whereas further deletion to −75 abolishes promoter activity in the root as well (*10, 11*). A palindromic sequence from the octopine synthase promoter, which also binds ASF-1, has been shown to confer root-specific expression when inserted upstream of a CaMV 35*S* promoter truncated at −46 (*21*). These data thus suggest that a single binding site for ASF-1 confers expression preferentially in root. In the present work, we show that addition of the *as-1* tetramer enhances leaf expression considerably (Fig. 1). We have reported previously that the steady-state amount of transcripts coding for ASF-1 is about ten times higher in root than in leaf (*22*). Together, these data suggest that the concentration of ASF-1 may be limiting in leaf as compared to root, and that the low concentration in leaf may be overcome by multimerization of the *as-1* binding site. However, these results do not exclude the possibility that ASF-1 exists in different forms in the two organs. Nevertheless, our present results show that *as-1* can confer leaf expression as well as root expression. The apparent dependence of tissue-specific expression on factor concentration and the copy number of its cognate binding site is similar to the recent observation with the *Drosophila* homeotic gene *bicoid* (*23*), and may reflect a basic principle by which diverse patterns of gene expression can be generated from a small set of differentially regulated factors.

REFERENCES

1. C. Kuhlemeier, P. J. Green, N.-H. Chua, *Annu. Rev. Plant. Physiol.* **38**, 221 (1987).
2. C. Dean, E. Pichersky, P. Dunsmuir, *ibid.* **40**, 415 (1989).
3. K. Aoyagi, C. Kuhlemeier, N.-H. Chua, *Mol. Gen. Genet.* **213**, 179 (1988).
4. J. Simpson, M. Van Montagu, L. Herrera-Estrella, *Science* **233**, 34 (1986).
5. P. J. Green, S. A. Kay, N.-H. Chua, *EMBO J.* **6**, 2543 (1987).
6. G. Giuliano *et al.*, *Proc. Natl. Acad. Sci. U.S.A.* **85**, 7089 (1988).
7. C. Kuhlemeier *et al.*, *ibid.*, p. 4662.
8. C. Kuhlemeier, G. Stritmatter, K. Ward, N.-H. Chua, *Plant Cell* **1**, 471 (1989).
9. P. N. Benfey and N.-H. Chua, *Science* **244**, 174 (1989).
10. C. Poulsen and N.-H. Chua, *Mol. Gen. Genet.* **214**, 16 (1988).
11. P. N. Benfey, L. Ren, N.-H. Chua, *EMBO J.* **8**, 2195 (1989).
12. P. J. Green *et al.*, *ibid.* **7**, 4035 (1988).
13. E. Lam, P. N. Benfey, P. Gilmartin, R.-X. Fang, N.-H. Chua, *Proc. Natl. Acad. Sci. U.S.A.* **86**, 7890 (1989).
14. R. T. Fraley *et al.*, *Bio/Technology* **3**, 629 (1985).
15. R. A. Jefferson, T. A. Kavanagh, M. W. Bevan, *EMBO J.* **6**, 3901 (1987).
16. R. Fluhr, P. M. Moses, G. Morelli, G. Coruzzi, N.-H. Chua, *ibid.* **5**, 2065 (1986).
17. E. Lam, unpublished data.

18. C. Kuhlemeier, R. Fluhr, P. J. Green, N.-H. Chua, *Genes Dev.* **1**, 247 (1987).
19. S. A. Johnston *et al.*, *Cell* **50**, 143 (1987).
20. P. K. Sorger and H. Pelham, *ibid.* **54**, 855 (1988).
21. H. Fromm, F. Katagiri, N.-H. Chua, *Plant Cell* **1**, 977 (1989).
22. F. Katagiri, E. Lam, N.-H. Chua, *Nature* **340**, 727 (1989).
23. G. Struhl, K. Struhl, P. M. Macdonald, *Cell* **57**, 1259 (1989).
24. We thank P. Green and P. Benfey for plasmids, H. Williams for photography, B. Niner for expert technical assistance, and P. Gilmartin for critical reading of the manuscript. E.L. was supported by a postdoctoral fellowship from NIH. This work was supported by Monsanto Co.

1 November 1989; accepted 8 March 1990

Ostwald Ripening of Clays and Metamorphic Minerals

DENNIS D. EBERL,* JAN ŚRODOŃ, MARTIN KRALIK, BRUCE E. TAYLOR, ZELL E. PETERMAN

Analyses of particle size distributions indicate that clay minerals and other diagenetic and metamorphic minerals commonly undergo recrystallization by Ostwald ripening. The shapes of their particle size distributions can yield the rate law for this process. One consequence of Ostwald ripening is that a record of the recrystallization process is preserved in the various particle sizes. Therefore, one can determine the detailed geologic history of clays and other recrystallized minerals by separating, from a single sample, the various particle sizes for independent chemical, structural, and isotopic analyses.

CLAY MINERALS GENERALLY HAVE large surface areas and exhibit a range of particle sizes. These characteristics suggest that clays may undergo Ostwald ripening (*1–6*) when exposed to fluids such as ground water or hydrothermal solutions, although this process must occur slowly at near-surface temperatures because clays are so insoluble. Recent evidence (*7, 8*) indicates that illite can recrystallize by Ostwald ripening in some hydrothermal systems. In this report we show that this process also occurs in other minerals and environments, and we discuss the effect that Ostwald ripening has on the crystal chemistry and geology of clays.

Ostwald ripening is a recrystallization process that is characterized by the simultaneous dissolution and growth of a mineral in a single medium. After nonexplosive nucleation, a system contains a great many crystallites of different sizes. Surface free energy then tends toward a minimum by the dissolution of small particles and the growth of large particles as matter is transferred from the former to the latter through solution (*4*). As ripening proceeds in a closed system, the mean crystallite size increases, the level of supersaturation in the solution decreases, the particle size distribution spreads out, and the number of particles decreases. As the level of supersaturation in solution decreases with increasing particle size, the mechanism of crystal growth may change from a process with a first-order reaction rate to one with a second-order rate (*4, 5*). Equilibrium cannot be attained until, by some process, the mineral consists of a single crystal or all the crystallites of a mineral are the same size. A complete record of the recrystallization process will be contained in the largest particle: it will be zoned progressively from an older core, representing the nucleation stage, to a younger rim, because the largest particles in the system never undergo dissolution (*4*). This history also will be preserved in the various particle sizes because the relative size relation between particles formed in the original nucleation step is maintained during ripening (*9*).

The occurrence of Ostwald ripening can be detected, and the mechanism that controlled the rate of the ripening process can be determined, from the particle size distribution, as originally suggested by Lifshitz and Slyozov (*10*) and Wagner (*11*). This quantitative description of Ostwald ripening is known as the LSW theory (*4*). Particle thickness distributions for three illites (Fig. 1) from shales from the Glarus Alps (*12*) show a sequence expected for ripening: mean particle thicknesses increase and particle thickness distributions spread out as metamorphic grade increases. In addition, the Alpine illites show convergence to a steady-state profile when particle thickness distributions are nondimensionalized (based on the use of reduced coordinates according to LSW theory; Fig. 2A); this is done by dividing by both the mean particle thickness for each distribution and the value for the maximum frequency in each distribution.

The occurrence of similar, reduced profiles (Fig. 2A) that approach a steady-state distribution (a distribution that is independent of the mean particle size and the initial, pre-recrystallization particle size distribution) is indirect proof that the clays have undergone Ostwald ripening (*4, 10*). Profiles having shapes similar to those found for the Alpine samples, but displaced toward larger reduced radii, also were found for

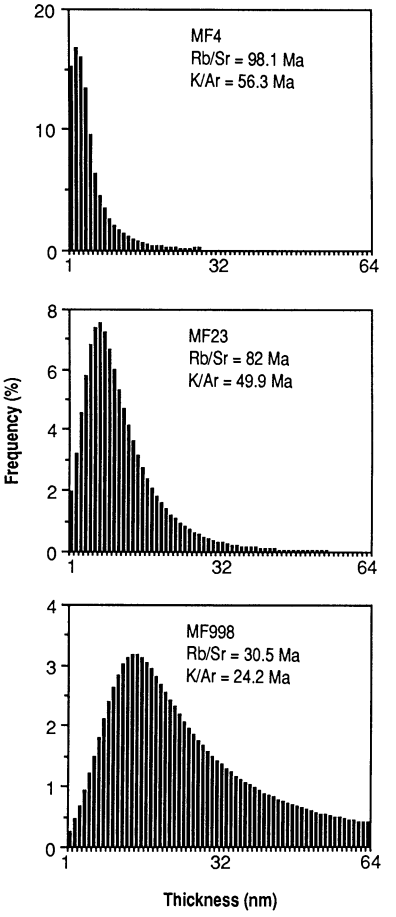

Fig. 1. Particle thickness distributions for illites from the Glarus Alps (*12*): metamorphic grade increases from sample MF4 (beginning of the anchizone) via MF23 to sample MF998 (epizone) on the basis of illite "crystallinity." Thickness measurements were made by the Warren-Averbach (W-A) technique (*14*), with Siemens D500 software, and the 002 and 005 x-ray diffraction peaks for Sr-saturated, <2-μm samples. Particle thicknesses measured by the W-A technique were checked by TEM measurements for five illite samples. The two techniques were found to give nearly identical mean particle thicknesses and particle thickness distributions. Ages are from (*12*).

D. D. Eberl, U.S. Geological Survey, Mail Stop 404, Federal Center, Denver, CO 80225.
J. Środoń, Institute of Geological Sciences, Polish Academy of Sciences, 31-002 Krakow, Senacka 3, Poland.
M. Kralik, Geotechnical Institute, Federal Testing and Research Institute–Arsenal, Faradayg, 3, Post Office Box 8, A-1030 Vienna, Austria.
B. E. Taylor, Geological Survey of Canada, 601 Booth Street, Ottawa, Ontario, Canada K1A 0E8.
Z. E. Peterman, U.S. Geological Survey, Mail Stop 963, Federal Center, Denver, CO 80225.

*To whom correspondence should be addressed.